Kynurenine-Induced Aryl Hydrocarbon Receptor Signaling in Mice Causes Body Mass Gain, Liver Steatosis, and Hyperglycemia

Itzel Y. Rojas[1], **Benjamin J. Moyer**[1], **Carol S. Ringelberg**[1], **Owen M. Wilkins**[1], **Darcy B. Pooler**[1,2], **Dylan B. Ness**[1,2], **Shodeinde Coker**[1,2,3], **Tor D. Tosteson**[1,2,4], **Lionel D. Lewis**[1,2,3], **Mary D. Chamberlin**[1,2,3], **Craig R. Tomlinson**[1,2,5]

[1]Norris Cotton Cancer Center, Dartmouth Hitchcock Medical Center, Lebanon, New Hampshire, USA.

[2]Geisel School of Medicine at Dartmouth, Dartmouth Hitchcock Medical Center, Lebanon, New Hampshire, USA

[3]Department of Medicine, Dartmouth Hitchcock Medical Center, Lebanon, New Hampshire, USA

[4]Department of Biomedical Data Science, Dartmouth Hitchcock Medical Center, Lebanon, New Hampshire, USA

[5]Department of Molecular & Systems Biology, Dartmouth Hitchcock Medical Center, Lebanon, New Hampshire, USA.

Abstract

Objective: The aryl hydrocarbon receptor (AHR) plays a key role in obesity. *In vitro* studies revealed that the tryptophan metabolite kynurenine (Kyn) activates AHR signaling in cultured hepatocytes. The objective of this study was to determine whether Kyn activated the AHR in mice to induce obesity.

Methods: Mice were fed a low-fat diet and the same diet supplemented with Kyn. Body mass, liver status, and the expression of identified relevant genes were determined.

Results: Kyn caused mice to gain significant body mass, develop fatty liver and hyperglycemia, and increase expression levels of cytochrome P450 1B1 and stearoyl-CoA desaturase 1. The hyperglycemia was accompanied with decreased insulin levels, which may have been due to the repression of genes involved in insulin secretion. Kyn plasma concentrations and BMI were measured in female patients, and a significant association was observed between Kyn and age in patients with obesity but not in patients who were lean.

Conclusions: Results show that (1) Kyn or a metabolite thereof is a ligand responsible for inducing AHR-based obesity, fatty liver, and hyperglycemia in mice; (2) plasma Kyn levels increase with age in women with obesity but not in lean women; and (3) an activated AHR is necessary but not sufficient to attain obesity, a status that also requires fat in the diet.

Introduction

The past several decades have seen a sharp increase in the prevalence of obesity (1). The pathology of obesity is multifactorial and dependent on genetics, environmental exposures, and behavior; thus, understanding the various biological mechanisms of obesity is important if an effective treatment strategy is to be developed. Several studies have shown that the aryl hydrocarbon receptor (AHR) is involved in diet-induced obesity (DIO) in mouse models (2–6). The AHR was first identified as the receptor for 2,3,7,8-tetrachlorodibenzo-*p*-dioxin (TCDD) and as a transcriptional inducer of the *Cyp1* gene family, which encodes enzymes that metabolize xenobiotics (7). Hundreds of confirmed and putative ligands for the AHR have been identified, most of which act as agonists to induce a variety of AHR-directed physiological functions, including roles in development (8) and immunity (9), as well as obesity. The *Ahr* gene knockout mouse is obesity resistant when fed a high-fat diet'(2,5), and the administration of the AHR antagonist alpha-naphthoflavone (aNF) or CH-223191 prevents (2,3,6) and reverses (6) DIO in male mice. The administration of a Western diet containing aNF also prevents DIO in female mice (3). Together, these studies suggest that AHR activation by a high-fat diet contributes to DIO and that AHR inhibition prevents and reverses obesity.

Kynurenine (Kyn) is a metabolite of tryptophan (Trp), of which 95% is catabolized via the Kyn pathway. The rate-limiting enzymes that convert Trp to Kyn are indole-2,3-dioxygenase 1 and 2 (IDO1 and IDO2, respectively) and tryptophan-2,3-dioxygenase 2 (TDO2). IDO1 dysregulation rather than that of IDO2 or TDO2 appears to be the primary cause of the disequilibrium of Kyn and Trp blood levels (10). IDO1 expression and activity are significantly greater in the adipose tissue and liver of women with obesity than those of lean women, and Kyn levels and the ratio of Kyn to Trp (Kyn/Trp) in the plasma of women with obesity are elevated compared with the levels in lean women (11,12), which is consistent with the notion that Kyn may contribute to the onset and maintenance of obesity, at least in women. Kyn can induce transcriptional AHR activity in a variety of cell types (13), including hepatocyte cell lines as demonstrated by increased levels of the canonical AHR gene target cytochrome P450 family 1 subfamily A member 1 (*Cyp1a1*) (2). In turn, *Ido1* gene expression is regulated in an AHR-dependent manner (14), creating a positive AHR-IDO1 feedback loop. The Kyn-induced AHR also plays a role in T cell differentiation to drive a suppressive regulatory T cell program (14). Knockout of the *Ido1* gene or inhibition of IDO1 in mice causes obesity resistance (2,10,15), and *in vitro* studies have linked low-density lipoproteins, IDO1, and Kyn-induced AHR signaling in a mouse hepatocyte cell line (2), supporting a role for an IDO1-Kyn-AHR axis in obesity.

In this report, the effect of Kyn on AHR activation and obesity was investigated *in vivo* by feeding mice a standard low-fat control diet with and without Kyn. We show that Kyn caused a significant gain in body mass when compared with mice fed a control diet alone.

Mice fed the control+Kyn diet exhibited increased hepatic fat deposition and adipocyte hypertrophy. The mice also exhibited higher plasma glucose concentrations without a corresponding decrease in fasting insulin. Analysis of liver mRNA revealed that Kyn repressed expression of genes that encode proteins for insulin secretion. In humans, we found that the relationship between Kyn and age was significant only in women with obesity. We conclude that the *in vivo* activation of the AHR via Kyn causes weight gain, liver steatosis, and disrupted plasma glucose regulation.

Methods

Mice

Male C57BL/6J (B6) mice (stock #000664) of approximately 5 weeks of age were purchased from The Jackson Laboratory (Bar Harbor, Maine). The mice were reared in 12-hour light/dark cycles. To minimize exposure to toxicants, cages were bedded with chemical-free shredded paper (Pure-o-cell, Maumee, Ohio). Food consumption was determined for an 8-day period midway during the diet regimens for each experimental group. Body mass of each mouse was recorded each week for the duration of a given study. For one study, mice were given 1-methyl-L-tryptophan (1MLT; Sigma-Aldrich, St. Louis, Missouri; CAS number 21339–55-9) in their drinking water (5 mg/mL, pH 11.0) or water adjusted to pH 11.0 for the control group (16). The studies were not blinded as the different chows were color coded. All mice *(Mus musculus)* were treated humanely following the regulations and specifications of the Dartmouth Hitchcock Medical Center Institutional Animal Care and Use Committee, Lebanon, New Hampshire. The studies were conducted using an animal protocol approved by the Dartmouth Hitchcock Medical Center Institutional Animal Care and Use Committee, protocol number toml.cr.1#2(m5ar5), assurance number A3259–01AQ13.

Diet

Mouse chow was purchased from Research Diets, Inc. (New Brunswick, New Jersey). The custom low-fat control diet (D12450B) contained 20% kilocalories from protein, 70% kilocalories from carbohydrates (35% kilocalories from sucrose), and 10% kilocalories from fat (4.5% kilocalories from lard). The custom Western diet (D12071702) contained 20% kilocalories from protein, 35% kilocalories from carbohydrates (17.5% kilocalories from sucrose), 45% kilocalories fat (40% kilocalories from lard), and 2% cholesterol. The control diet contained 3.8 kcal/g, and the Western diet contained 4.6 kcal/g (3). The ingredients for the control and Western diets were listed previously (3). Kyn (Sigma-Aldrich) was incorporated (125 mg/kg chow) into the control diet during manufacturing at Research Diets. Trp amounts were equal among the chows and there was no measurable Kyn in the control and Western diets.

Histology

Liver and adipose tissue were harvested at sacrifice following perfusion with phosphate-buffered saline (PBS) and then were fixed in 4% paraformaldehyde (Sigma-Aldrich). Further details regarding the histology methods can be found in the accompanying online Supporting Information.

Western blotting

Lysate protein concentrations were determined, and the proteins were resolved by sodium dodecyl sulfate (SDS)-polyacrylamide gel electrophoresis (PAGE) under reduced conditions and transferred to polyvinylidene difluoride membrane (EMD Millipore, Burlington, Massachusetts). Further details regarding Western blotting are in the online Supporting Information.

Enzyme-linked immunosorbent assays for secreted phosphoprotein and insulin

Blood was obtained from mice at sacrifice via cardiac puncture. Plasma was separated via centrifugation and stored at −80°C. Further details regarding the enzyme-linked immunosorbent assays (ELISA) are in the online Supporting Information.

Determination of Kyn, Trp, and arachidonic acid plasma concentrations

Plasma was obtained by centrifugation from collected blood samples and stored at −80°C. High-performance liquid chromatography (HPLC) tandem mass spectrometry was carried out by the Dartmouth Clinical Pharmacology Shared Resource. Further details regarding these assays are in the online Supporting Information.

Oral glucose tolerance test

Mice were fasted for 6 hours prior to receiving an oral bolus of 2 g of glucose (Sigma-Aldrich) per kilogram of body weight. Fasting glucose was measured at time zero using a OneTouch Glucometer (LifeScan, Chesterbrook, Pennsylvania) and at selected time points over the course of 120 minutes. Blood for the assays was taken from the tail. The glucose challenge was performed on the mice at 10 to 12 weeks in the 20-week diet regimen, ensuring a sufficient recovery period by the time the study was terminated.

Microarrays

Four biological replicates per experimental condition were used for the microarray studies. Further details regarding the microarray methods are in the online Supporting Information.

Human studies

To determine whether Kyn may be associated with obesity in humans, a companion blood collection prospective study was carried out. Samples were analyzed from 60 female patients requiring routine breast or abdominal surgery for benign or malignant conditions. All participants provided written informed consent. The study protocol was reviewed and approved by the Committee for Protection of Human Safety at Dartmouth College. Further details regarding the human studies are in the online Supporting Information.

Data analysis

Microarray analyses were performed using BRB-Array Tools version 4.5 (Biometric Research Program of the National Cancer Institute). For the human data, univariate linear regression was used to assess relationships among continuous variables in the study population (e.g., patient age, BMI, Kyn plasma levels). Further details regarding the data analyses are in the online Supporting Information.

Results

Kyn induces body mass gain

We and others have shown that loss of *Ido1* gene function causes obesity resistance in B6 mice fed high-fat diets (2,10) and that Kyn acts as an AHR agonist *in vitro* (2,14,15). Here we asked whether Kyn plays an *in vivo* role in AHR-based obesity. Male B6 mice were fed a control diet (low fat), control diet supplemented with Kyn (to provide ~16.7 mg/kg body mass/d), or a high-fat Western diet for 20 weeks. Mice fed the control diet+Kyn gained 15% more body mass than mice fed the control diet alone, and as expected, mice on the Western diet more than doubled their weight gain compared with that of mice on the control diet (Figure 1A). Weight gain from Kyn was not due to increased caloric consumption as there was no significant difference between the control and control+Kyn diet groups in the amount of kilocalories consumed (Figure 1B) or in food gram intake (data not shown). Kyn caused a small but statistically significant drop in liver mass to body mass ratio and, as expected from previous studies (2,3,6), the Western diet caused an increase in relative liver mass (Figure 1C). Most of the body mass gain in mice of the control+Kyn diet group was from increased fat deposition in subcutaneous adipose tissue (SCAT), and as has been observed in past work (2), fat deposition occurred in both visceral adipose tissue (VAT) and SCAT depots for the mice on the Western diet (Figure 1C). Adipose tissue expansion occurs via two mechanisms: hypertrophy (adipocyte enlargement) and/or hyperplasia (increased adipocyte cell division). We found via hematoxylin and eosin staining that the inguinal (SCAT) and epididymal (VAT) fat depots of mice fed the control+Kyn diet displayed increased hypertrophic growth relative to that of mice fed the control diet but to a lesser extent than that of mice fed the Western diet (Figure 1D), which suggests that Kyn caused an induction of adipose lipid transport and storage.

If the increased dietary intake of Kyn exerts a physiological effect, then it would be expected that plasma levels of Kyn would correspondingly increase. The supplemented Kyn was indeed absorbed in greater amounts in the experimental group, as plasma Kyn levels and the Kyn/Trp ratio were significantly higher in the control+Kyn group relative to the mice fed control and Western diets (Figure 1E), and the Kyn/Trp ratio was more similar to that of mice on the Western diet (Figure 1F). The compound 1MLT inhibits IDO1 enzymatic activity and affects body mass. To confirm that IDO1 may be playing a role here, male B6 mice were administered drinking water with and without 1MLT (5 mg/mL) for 14 weeks. The group that received 1MLT gained significantly less body weight (Figure 1G). These results are consistent with a model depicting Kyn or a Kyn metabolite as an *in vivo* inducer of AHR-based obesity.

Kyn causes hepatic steatosis and increased liver *Cyp1b1* and *Scd1* gene expression

The canonical AHR-regulated *Cyp1b1* gene (7) is expressed in most tissues (17) and is transcriptionally induced by the AHR (18). Like the *Ahr* gene knockout mouse (2,5,19), the *Cyp1b1* gene knockout mouse on a high-fat diet is obesity resistant (20,21). The *Cyp1b1* gene is induced in the liver and adipose tissue of B6 mice fed a Western diet (6); in contrast, obesity, liver steatosis, and *Cyp1b1* expression are at control levels in mice fed a Western diet containing the AHR antagonist aNF (6).

We found that hepatic lipid deposition increased in mice fed a control+Kyn diet compared with mice fed a control diet, with the number of fat-storing vesicles approaching what was observed in mice fed a Western diet (Figure 2A). Although mRNA levels were not affected, there was a concomitant increase in hepatic cytochrome P450 1B1 (CYP1B1) protein expression in mice on the control+Kyn diet, again similar to what was observed in the liver of mice fed a Western diet (Figure 2B). The AHR is known to be active in perivenous hepatocytes (6), and CYP1B1 is expressed exclusively in perivenous hepatocytes after chronic TCDD exposure (22). Similarly, CYP1B1 staining of the liver from mice fed a control+Kyn diet was markedly increased relative to that of control mice, and like the liver from Western diet–fed mice, staining was exclusively in the perivenous hepatocytes (Figure 2C).

Obesity can be restored in the *Cyp1b1* knockout mouse with virus-expressing stearoyl-CoA desaturase 1 (SCD1) (20), an enzyme that converts saturated fatty acids to monounsaturated fatty acids. We had reported that consumption of a Western diet increased *Scd1* and peroxisome proliferator-activated receptor alpha (PPARα)-target gene mRNA and protein expression in liver relative to that of mice on a control diet, and that inhibition of the AHR led to a reduction of *Scd1* and PPARα-target gene expression (6). Like B6 mice fed a Western diet, mice fed a control+Kyn diet showed increased mRNA levels of *Scd1* (Figure 2D) and some PPARα-target genes, including *Scd1* (Table 1), relative to mice fed a control diet.

We investigated the effect of Kyn on the expression of osteopontin (secreted phosphoprotein 1; SPP1), an obesity-associated cytokine that is induced by the AHR (23). We reported that *Spp1* mRNA expression in liver and adipose tissue and SPP1 plasma protein levels increased significantly in B6 mice fed a Western diet but remained at control levels when the AHR antagonist aNF was included in the diet (6). Western diet–fed mice exhibited increased hepatic *Spp1* mRNA levels, but there was no significant change relative to mice fed a control+Kyn diet (Figure 2E). These results support the contention that Kyn may induce AHR-directed expression of the *Cyp1b1* and *Scd1* genes but not the *Spp1* gene.

Kyn alters gene expression of lipid metabolism and redox pathways

We performed microarray analysis on liver mRNA from mice fed control and control+Kyn diets, which revealed that lipid metabolism was the predicted biological pathway most significantly altered (Table 2). Free fatty acids in the liver are derived from diet, *de novo* lipogenesis (DNL), and/or increased lipolysis in adipose tissue from which free fatty acids are transported to the liver (24). Because there were no differences in dietary fat amounts between the control and control+Kyn diets, the altered expression of genes involved in lipid synthesis and transcription from the microarray results (Table 2) are consistent with the idea that the Kyn-activated AHR regulates genes that regulate liver DNL. Furthermore, the adipose tissue in the Kyn-treated mice showed increased fat stores (Figure 1D).

The top differentially expressed genes in liver shared by mice fed Western and control+Kyn diets were found to be members of the oxidation reduction (redox) pathway (Table 3). Hepatic redox dysfunction is implicated in the progression of several diseases, including nonalcoholic fatty liver disease (NAFLD) (25). Liver *Scd1* gene expression, which changed

similarly in mice fed Western and control+Kyn diets (Figure 2D), was the top differentially expressed gene in the redox pathway. These results suggest that the DNL and redox gene programs are transcriptionally regulated by the Kyn-activated AHR to cause fatty liver.

Kyn disrupts glucose homeostasis

Because type 2 diabetes is associated with obesity, we investigated whether mice treated with Kyn displayed impaired glucose homeostasis. Oral administration of a glucose bolus showed that increased Kyn consumption caused a sustained increase in circulating plasma glucose in that plasma glucose levels were significantly higher at every measured time point of the subsequent 2-hour duration (Figure 3A) and as measured by the total area under the curve (Figure 3B). Plasma insulin levels were measured in mice at sacrifice at the conclusion of the 20-week diet regimen, and as expected, mice fed a Western diet had significantly greater levels of plasma insulin relative to that of mice fed the control diet (Figure 3C). However, mice fed the control+Kyn diet displayed fasting insulin levels that were lower but not statistically different than that of mice fed the control diet.

Glucose stimulates production of arachidonic acid as well as insulin (26). Arachidonic acid causes a decrease in *Scd1* mRNA and activity levels (27) and it is a substrate for CYP1B1, providing a variety of potent bioactive eicosanoids (28), which include AHR agonists (29). Furthermore, we have shown a significant drop in plasma arachidonic acid levels to near control levels in mice fed a Western diet containing an AHR antagonist relative to mice fed a Western diet alone (6). The inclusion of Kyn in the control diet caused a substantial but nonsignificant increase in plasma arachidonic acid levels (Figure 3D). The results show that Kyn administration causes higher plasma levels of glucose and arachidonic acid and lower levels of insulin.

Kyn affects gene expression for lipid metabolism, insulin resistance, and glucose homeostasis but not inflammation

The obesity-linked onset of insulin resistance is associated with chronic, low-grade inflammation due to the secretion of proinflammatory cytokines from hypertrophic adipose tissue, the latter a Kyn-inducible condition (Figure 1C–1D). Chronic inflammation leads to proinflammatory signaling in the liver that abrogates hepatic insulin sensitivity. Differential gene expression profiles of liver genes from mice fed a control+Kyn diet compared with mice fed a control diet (Table 4, right column) revealed that Kyn influenced the expression of genes involved in insulin secretion and glucose responsiveness. Notably, treatment with Kyn caused the downregulation of genes involved in the positive regulation of insulin secretion and the upregulation of genes in networks that govern the physiological response to glucose. Furthermore, Kyn had no significant effect on the genes that participate in hepatic inflammation in contrast with that of mice fed a Western diet (Table 4, middle column). Most of the Kyn-affected genes were independent of those genes affected by a Western diet; however, a major exception was genes involved in lipid metabolism, in which both groups showed very similar gene expression profiles. The results suggest that it is primarily the Kyn-activated AHR in DIO that regulates the genes involved in lipid metabolism. AHR activation by Kyn and the Western diet was similar in that both diets affected genes involved in lipid metabolism but was dissimilar in that Kyn singularly

affected gene programs involved in the regulation of hyperglycemia and insulin levels independently of an inflammatory state.

Kyn plasma concentrations are dependent on age in humans with obesity

Plasma Kyn levels have been associated with obesity (11,12) and age (30,31) in humans. Plasma samples were collected from 60 female patients from whom age, BMI, and Kyn plasma levels were recorded. Kyn plasma levels were not different in women stratified as being lean and having overweight (BMI = 19 to < 30) (Figure 4A, left) versus having obesity (BMI = 30) (Figure 4A, right); however, a significant association between Kyn and age was observed in women with obesity. That is, the absolute levels of Kyn were not different between the groups, but a positive association for age and BMI was seen in the obesity cohort. As expected, Kyn levels were significantly associated in a positive direction with Trp levels in women with both lean/overweight and obesity (Figure 4B), but the relationship of Trp with age did not reach significance in either the leaner patients or those with obesity (Figure 4C). As observed with Kyn, Kyn/Trp ratios demonstrated a significant age-dependent increase in women with obesity only, further supporting the age-dependent relationship observed for Kyn in women with obesity (Figure 4D). BMI and age were modestly associated, with BMI rising slightly as age increased (Figure 4E). Moreover, because there was no difference in the absolute levels of Kyn in plasma between lean patients/patients with overweight and patients with obesity, BMI and Kyn were not significantly associated (Figure 4F). These results support the contention that Kyn plasma levels are dependent on age only for those who have obesity. These data present a model for a possible relationship between Kyn levels and obesity in humans.

Discussion

We propose that Kyn and/or a metabolite(s) of Kyn causes significant body mass gain, hypertrophic adipose growth, and hyperglycemia via activation of the AHR. Induction of AHR signaling is supported by the appearance of CYP1B1 in the liver of mice fed a control+Kyn diet (Figure 2B–2C). AHR activation by Kyn or a metabolite may be a necessary but insufficient means for development of obesity, in that, not surprisingly, an excess caloric consumption is likely also required for a full manifestation of obesity. The Kyn-induced AHR signaling resembles the so-called "normal obesity" state, in which a normal-range BMI is maintained but the individual displays increased levels of visceral adiposity, insulin resistance, and dyslipidemia (32), and an overly activated AHR in lieu of a high-caloric diet may serve as a mechanism for "normal obesity."

Another study concluded that the administration of Kyn to mice had no obesogenic effects (15). However, there were several key differences in that study compared with the one reported here. First, our study combined Kyn with a low-fat diet, whereas the other study included Kyn with a high-fat diet. Although our study showed that Kyn-induced AHR signaling resulted in a relatively modest but significant body mass gain, it is likely in the other study that any obesogenic effects from Kyn would have been overwhelmed by the presumed greater contribution to obesity by dietary fat. Second, we incorporated Kyn into

the chow as the route of administration rather than the drinking water, a route by which mice may consume relatively smaller amounts of Kyn or by which Kyn may have less effect.

Our studies showed that mice fed a control+Kyn diet had increased subcutaneous and visceral adiposity (Figure 1C). Higher volumes of VAT tend to become dysfunctional and contribute to the onset of metabolic syndrome, including NAFLD (33), whereas increased SCAT amounts are generally considered to have a relatively neutral impact on the metabolic state. Further studies are needed to determine whether chronic activation of the AHR indeed prepares the liver and adipose tissue for storing excess fat in obesity.

Our previous work in AHR-based DIO demonstrated a crucial role for the AHR target gene *Cyp1b1* (3,6). Here, we found that Kyn upregulated the expression of *Cyp1b1* in the liver (Figure 2), in synchrony with increased hepatic lipid deposition. The expression of liver *Scd1* mRNA was also upregulated by Kyn. As with the *Cyp1b1* gene knockout mouse (20,21), the *Scd1* gene knockout mouse is protected from DIO, hepatic steatosis, and adiposity (34,35), and decreased liver triglyceride deposition (36); additionally, the repression of hepatic SCD1 activity prevents liver injury. The studies here support a Kyn-activated AHR mechanism for obesity, mediated by the increased expression of *Cyp1b1* and *Scd1*. Lipidomic profiling of Kyn-treated animals and studies investigating Kyn exposure to *Cyp1b1*- and *Scd1*-null animals will further illuminate the role of Kyn in obesity.

Obesity is frequently accompanied by metabolic syndrome, characteristics that include hyperglycemia and insulin resistance. We showed that activation of the AHR by Kyn resulted in postprandial hyperglycemia (Figure 3A–3B). The sustained elevation of plasma glucose in mice fed a control+Kyn diet approached that of mice fed a Western diet; however, control+Kyn–fed mice did not have the parallel increase in fasting plasma insulin levels (Figure 3C). Although use of the pancreas would have been preferable, the microarray data from the liver provided possible insight by identifying genes involved in insulin secretion and responsiveness, which were downregulated and upregulated, respectively, by Kyn intake (Table 3). Downregulation of insulin secretion and upregulation of insulin/glucose responsiveness liver genes suggest that AHR-directed hyperglycemia is not due to insulin resistance, which presents elevated plasma insulin levels. Insulin acts to regulate glucose availability by increasing glucose uptake in muscle, suppressing gluconeogenesis in liver, and promoting glucose uptake and inhibiting lipolysis in adipose tissue. Studies have disclosed opposing functions of the AHR in the insulin response, in that constitutive activity of the AHR (37) as well as the loss of the AHR (19) improves insulin sensitivity. An apparent consensus on the issue is that the effect of the AHR on insulin sensitivity is ligand-dependent (38), and our results suggest that the Kyn-activated AHR may participate in this dichotomy by promoting a hyperglycemic state via repression of genes involved in insulin secretion.

Other studies showed that knockout of the *Ahr* gene in mice caused decreased glucose tolerance, increased plasma insulin levels, and decreased PPARα activity (19), which nicely contrast with the data shown here, in which Kyn activated the AHR to cause increased glucose tolerance, decreased insulin levels, and induced PPARα signaling (Table 1; Figure 3). These outcomes support an association among the AHR, PPARα, glucose tolerance, and

insulin sensitivity, for which Kyn may be the instigator. Arachidonic acid is also associated with obesity by affecting inflammation and augmenting liver steatosis in obese mice and in humans, in which higher plasma levels of arachidonic acid-derived metabolites are linked to obesity (39). We showed that mice on a control+Kyn diet displayed a considerable increase in plasma arachidonic acid levels (Figure 3D), which suggests that the Kyn-activated AHR may lead to an increased production of arachidonic acid, which in turn may contribute to fatty liver.

NAFLD is linked to obesity, and dysfunction in hepatic redox homeostasis and increased oxidative stress are implicated in the pathogenesis of NAFLD (40). Microarray analysis of liver mRNA from mice treated with Kyn highlighted an increase in genes related to redox function, similar to the increase observed in mice fed a Western diet (Table 3). This, and an increase in active lipid metabolism gene networks (Table 2), suggests that AHR activation by Kyn creates an environment that upregulates DNL, which suggests DNL underlies ectopic lipid deposition. The top differentially expressed gene in mouse liver was regulator of G-protein signaling 16 (RGS16) (3.80-fold and 4.56-fold, respectively). RGS16 is implicated in hepatic energy sensing, and *Rgs16* gene expression in the liver is associated with increased triglyceride content (41), which suggests another possible downstream effector for AHR-mediated fatty liver deposition.

In humans, increased IDO1 activity and higher Kyn plasma concentrations have been positively correlated to older age (31), although gender and disease state may also play roles. Increased IDO activity is linked to higher mortality in humans (42), and an increased Kyn/Trp ratio is associated with human frailty (43). We found that in women (ages 18–75), increased age positively correlated with obesity and rising Kyn plasma levels (Figure 4). *Ido1* gene expression and activity are regulated by the AHR (14) as well as by IFNγ and TNFα, which originate from the chronic inflammation associated with obesity and older age (44). Thus, we hypothesize that in older females with obesity, the heightened inflammation and increasing Kyn levels cooperatively form positive feedback loops, causing increased activation of the AHR in liver and adipose (6) to amplify the obesity state. Furthermore, it was shown that physical exercise, a more common activity of leaner and younger women, increased skeletal muscle expression of kynurenine aminotransferase to shift the metabolism of Kyn to kynurenic acid, which lowered Kyn plasma levels (45). The observation that the relationship between age and Kyn levels is specific to women with obesity suggests that the obesity promoting effects of Kyn may be restricted to older women; however, more studies are required to delineate cause and effect between Kyn and obesity in human populations.

In conclusion, by treating mice with Kyn, we identified a likely food-derived, *in vivo* agonist for AHR-based obesity. The Kyn-activated AHR caused an increase in body mass, adiposity, hepatic lipid deposition, and the disruption of glucose homeostasis. Although we cannot demonstrate cause and effect, the association observed between Kyn and obesity may manifest in an age-dependent fashion in humans. The IDO1-Kyn-AHR axis warrants further investigation as a possible therapeutic target in the treatment of obesity.

Supplementary Material

Refer to Web version on PubMed Central for supplementary material.

Acknowledgments

References

1. GBD 2015 Obesity Collaborators; Afshin A, Forouzanfar MH, Reitsma MB, et al. Health effects of overweight and obesity in 195 countries over 25 years. N Engl J Med 2017;377:13–27. [PubMed: 28604169]

2. Moyer BJ, Rojas IY, Kerley-Hamilton JS, et al. Inhibition of the aryl hydrocarbon receptor prevents Western diet-induced obesity. Model for AHR activation by kynurenine via oxidized-LDL, TLR2/4, TGFbeta, and IDO1. Toxicol Appl Pharmacol 2016;300:13–24. [PubMed: 27020609]

3. Moyer BJ, Rojas IY, Kerley-Hamilton JS, et al. Obesity and fatty liver are prevented by inhibition of the aryl hydrocarbon receptor in both female and male mice. Nutr Res 2017;44:38–50. [PubMed: 28821316]

4. Kerley-Hamilton JS, Trask HW, Ridley CJ, et al. Obesity is mediated by differential aryl hydrocarbon receptor signaling in mice fed a Western diet. Environ Health Perspect 2012;120:1252–1259. [PubMed: 22609946]

5. Xu CX, Wang C, Zhang ZM, et al. Aryl hydrocarbon receptor deficiency protects mice from diet-induced adiposity and metabolic disorders through increased energy expenditure. Int J Obes (Lond) 2015;39:1300–1309. [PubMed: 25907315]

6. Rojas IY, Moyer BJ, Ringelberg CS, Tomlinson CR. Reversal of obesity and liver steatosis in mice via inhibition of aryl hydrocarbon receptor and altered gene expression of CYP1B1, PPARα, SCD1, and osteopontin. Int J Obes (Lond) 2020;44:948–963. [PubMed: 31911663]

7. Nebert DW, Puga A, Vasiliou V. Role of the Ah receptor and the dioxin-inducible [Ah] gene battery in toxicity, cancer, and signal transduction. Ann N Y Acad Sci 1993;685:624–640. [PubMed: 8395783]

8. Lahvis GP, Lindell SL, Thomas RS, et al. Portosystemic shunting and persistent fetal vascular structures in aryl hydrocarbon receptor-deficient mice. Proc Natl Acad Sci U S A 2000;97:10442–10447. [PubMed: 10973493]

9. Quintana FJ, Sherr DH. Aryl hydrocarbon receptor control of adaptive immunity. Pharmacol Rev 2013;65:1148–1161. [PubMed: 23908379]

10. Nagano J, Shimizu M, Hara T, et al. Effects of indoleamine 2,3-dioxygenase deficiency on high-fat diet-induced hepatic inflammation. PLoS One 2013;8:e73404. doi:10.1371/journal.pone.0073404 [PubMed: 24039933]

11. Wolowczuk I, Hennart B, Leloire A, et al. Tryptophan metabolism activation by indoleamine 2,3-dioxygenase in adipose tissue of obese women: an attempt to maintain immune homeostasis and vascular tone. Am J Physiol Regul Integr Comp Physiol 2012;303:R135–R143. [PubMed: 22592557]

12. Favennec M, Hennart B, Caiazzo R, et al. The kynurenine pathway is activated in human obesity and shifted toward kynurenine monooxygenase activation. Obesity (Silver Spring) 2015;23:2066–2074. [PubMed: 26347385]

13. Nguyen NT, Kimura A, Nakahama T, et al. Aryl hydrocarbon receptor negatively regulates dendritic cell immunogenicity via a kynurenine-dependent mechanism. Proc Natl Acad Sci U S A 2010;107:19961–19966. [PubMed: 21041655]

14. Mezrich JD, Fechner JH, Zhang X, Johnson BP, Burlingham WJ, Bradfield CA. An interaction between kynurenine and the aryl hydrocarbon receptor can generate regulatory T cells. J Immunol 2010;185:3190–3198. [PubMed: 20720200]

15. Laurans L, Venteclef N, Haddad Y, et al. Genetic deficiency of indoleamine 2,3-dioxygenase promotes gut microbiota-mediated metabolic health. Nat Med 2018;24:1113–1120. [PubMed: 29942089]

16. Takamatsu M, Hirata A, Ohtaki H, et al. Inhibition of indoleamine 2,3-dioxygenase 1 expression alters immune response in colon tumor microenvironment in mice. Cancer Sci 2015;106:1008–1015. [PubMed: 26033215]

17. Shimada T, Hayes CL, Yamazaki H, et al. Activation of chemically diverse procarcinogens by human cytochrome P-450 1B1. Cancer Res 1996;56:2979–2984. [PubMed: 8674051]

18. Galván N, Teske DE, Zhou G, et al. Induction of CYP1A1 and CYP1B1 in liver and lung by benzo(a)pyrene and 7,12-d imethylbenz(a)anthracene do not affect distribution of polycyclic hydrocarbons to target tissue: role of AhR and CYP1B1 in bone marrow cytotoxicity. Toxicol Appl Pharmacol 2005;202:244–257. [PubMed: 15667830]

19. Wang C, Xu C-X, Krager SL, Bottum KM, Liao D-F, Tischkau SA. Aryl hydrocarbon receptor deficiency enhances insulin sensitivity and reduces PPAR-α pathway activity in mice. Environ Health Perspect 2011;119:1739–1744. [PubMed: 21849270]

20. Li F, Jiang C, Larsen MC, et al. Lipidomics reveals a link between CYP1B1 and SCD1 in promoting obesity. J Proteome Res 2014;13:2679–2687. [PubMed: 24684199]

21. Liu X, Huang T, Li L, et al. CYP1B1 deficiency ameliorates obesity and glucose intolerance induced by high fat diet in adult C57BL/6J mice. Am J Transl Res 2015;7:761–771. [PubMed: 26064443]

22. Walker NJ, Crofts FG, Li Y, et al. Induction and localization of cytochrome P450 1B1 (CYP1B1) protein in the livers of TCDD-treated rats: detection using polyclonal antibodies raised to histidine-tagged fusion proteins produced and purified from bacteria. Carcinogenesis 1998;19:395–402. [PubMed: 9525272]

23. Chuang CY, Chang H, Lin P, et al. Up-regulation of osteopontin expression by aryl hydrocarbon receptor via both ligand-dependent and ligand-independent pathways in lung cancer. Gene 2012;492:262–269. [PubMed: 22037483]

24. Liu X, Yu L, Hassan W, Sun L, Zhang L, Jiang Z. The duality of Kupffer cell responses in liver metabolic states. Curr Mol Med 2016;16:809–819. [PubMed: 27804861]

25. Gambino R, Musso G, Cassader M. Redox balance in the pathogenesis of nonalcoholic fatty liver disease: mechanisms and therapeutic opportunities. Antioxid Redox Signal 2011;15:1325–1365. [PubMed: 20969475]

26. Turk J, Colca JR, Kotagal N, McDaniel ML. Arachidonic acid metabolism in isolated pancreatic islets. II. The effects of glucose and of inhibitors of arachidonate metabolism on insulin secretion and metabolite synthesis. Biochim Biophys Acta 1984;794:125–136. [PubMed: 6428455]

27. Sessler AM, Kaur N, Palta JP, Ntambi JM. Regulation of stearoyl-CoA desaturase 1 mRNA stability by polyunsaturated fatty acids in 3T3-L1 adipocytes. J Biol Chem 1996;271:29854–29858. [PubMed: 8939925]

28. Seidel SD, Winters GM, Rogers WJ, et al. Activation of the Ah receptor signaling pathway by prostaglandins. J Biochem Mol Toxicol 2001;15:187–196. [PubMed: 11673847]

29. Chiaro CR, Patel RD, Perdew GH. 12(R)-Hydroxy-5(Z),8(Z),10(E),14(Z)-eicosatetraenoic acid [12(R)-HETE], an arachidonic acid derivative, is an activator of the aryl hydrocarbon receptor. Mol Pharmacol 2008;74:1649–1656. [PubMed: 18779363]

30. Mangge H, Summers KL, Meinitzer A, et al. Obesity-related dysregulation of the tryptophan-kynurenine metabolism: role of age and parameters of the metabolic syndrome. Obesity (Silver Spring) 2014;22:195–201. [PubMed: 23625535]

31. Kaiser H, Yu K, Pandya C, et al. Kynurenine, a tryptophan metabolite that increases with age, induces muscle atrophy and lipid peroxidation. Oxid Med Cell Longev 2019;2019:9894238. doi:10.1155/2019/9894238

32. Franco LP, Morais CC, Cominetti C. Normal-weight obesity syndrome: diagnosis, prevalence, and clinical implications. Nutr Rev 2016;74:558–570. [PubMed: 27473199]

33. Milic S, Lulic D, Stimac D. Non-alcoholic fatty liver disease and obesity: biochemical, metabolic and clinical presentations. World J Gastroenterol 2014;20:9330–9337. [PubMed: 25071327]

34. Miyazaki M, Flowers MT, Sampath H, et al. Hepatic stearoyl-CoA desaturase-1 deficiency protects mice from carbohydrate-induced adiposity and hepatic steatosis. Cell Metab 2007;6:484–496. [PubMed: 18054317]

35. Ntambi JM, Miyazaki M, Stoehr JP, et al. Loss of stearoyl-CoA desaturase-1 function protects mice against adiposity. Proc Natl Acad Sci U S A 2002;99:11482–11486. [PubMed: 12177411]

36. Miyazaki M, Dobrzyn A, Sampath H, et al. Reduced adiposity and liver steatosis by stearoyl-CoA desaturase deficiency are independent of peroxisome proliferator-activated receptor-alpha. J Biol Chem 2004;279:35017–35024. [PubMed: 15180999]

37. Lu P, Yan J, Liu K, et al. Activation of aryl hydrocarbon receptor dissociates fatty liver from insulin resistance by inducing fibroblast growth factor 21. Hepatology 2015;61:1908–1919. [PubMed: 25614121]

38. Denison MS, Soshilov AA, He G, DeGroot DE, Zhao B. Exactly the same but different: promiscuity and diversity in the molecular mechanisms of action of the aryl hydrocarbon (dioxin) receptor. Toxicol Sci 2011;124:1–22. [PubMed: 21908767]

39. Pickens CA, Sordillo LM, Zhang C, Fenton JI. Obesity is positively associated with arachidonic acid-derived 5- and 11-hydroxyeicosatetraenoic acid (HETE). Metabolism 2017;70:177–191. [PubMed: 28403941]

40. Spahis S, Delvin E, Borys JM, Levy E. Oxidative stress as a critical factor in nonalcoholic fatty liver disease pathogenesis. Antioxid Redox Signal 2017;26:519–541. [PubMed: 27452109]

41. Pashkov V, Huang J, Parameswara VK, et al. Regulator of G protein signaling (RGS16) inhibits hepatic fatty acid oxidation in a carbohydrate response element-binding protein (ChREBP)-dependent manner. J Biol Chem 2011;286:15116–15125. [PubMed: 21357625]

42. Pertovaara M, Raitala A, Lehtimaki T, et al. Indoleamine 2,3-dioxygenase activity in nonagenarians is markedly increased and predicts mortality. Mech Ageing Dev 2006;127:497–499. [PubMed: 16513157]

43. Valdiglesias V, Marcos-Pérez D, Lorenzi M, et al. Immunological alterations in frail older adults: A cross sectional study. Exp Gerontol 2018;112:119–126. [PubMed: 30240849]

44. Chung HY, Kim DH, Lee EK, et al. Redefining chronic inflammation in aging and age-related diseases: proposal of the senoinflammation concept. Aging Dis 2019;10: 367–382. [PubMed: 31011483]

45. Dadvar S, Ferreira DMS, Cervenka I, Ruas JL. The weight of nutrients: kynurenine metabolites in obesity and exercise. J Intern Med 2018;284:519–533. [PubMed: 30141532]

Study Importance

What is already known?

- Kynurenine (Kyn) induces transcriptional aryl hydrocarbon receptor (AHR) activity in hepatocyte cell lines.

- Inhibition of the AHR prevents and reverses obesity and nonalcoholic fatty liver disease (NAFLD) in mice fed a high-fat diet.

- The cytochrome P450 1B1 (*Cyp1b1*), peroxisome proliferator-activated receptor alpha (*Ppara*), stearoyl-CoA desaturase 1 (*Scd1*), and secreted phosphoprotein 1 (*Spp1*) genes are involved in AHR-based obesity.

What does this study add?

- Addition of Kyn to a low-fat diet caused significant body mass gain and liver steatosis.

- The Kyn-activated AHR induced expression of CYP1B1 in perivenous hepatocytes and liver *Scd1* mRNA levels.

- Kyn-fed mice displayed higher plasma glucose and lower insulin levels, possibly from repression of insulin-secreting genes.

- In humans, Kyn plasma concentrations rose significantly with increasing age in women with obesity but not lean women.

How might these results change the direction of research or the focus of clinical practice?

- Reducing Kyn and AHR signaling levels may offer a potential treatment for obesity and NAFLD.
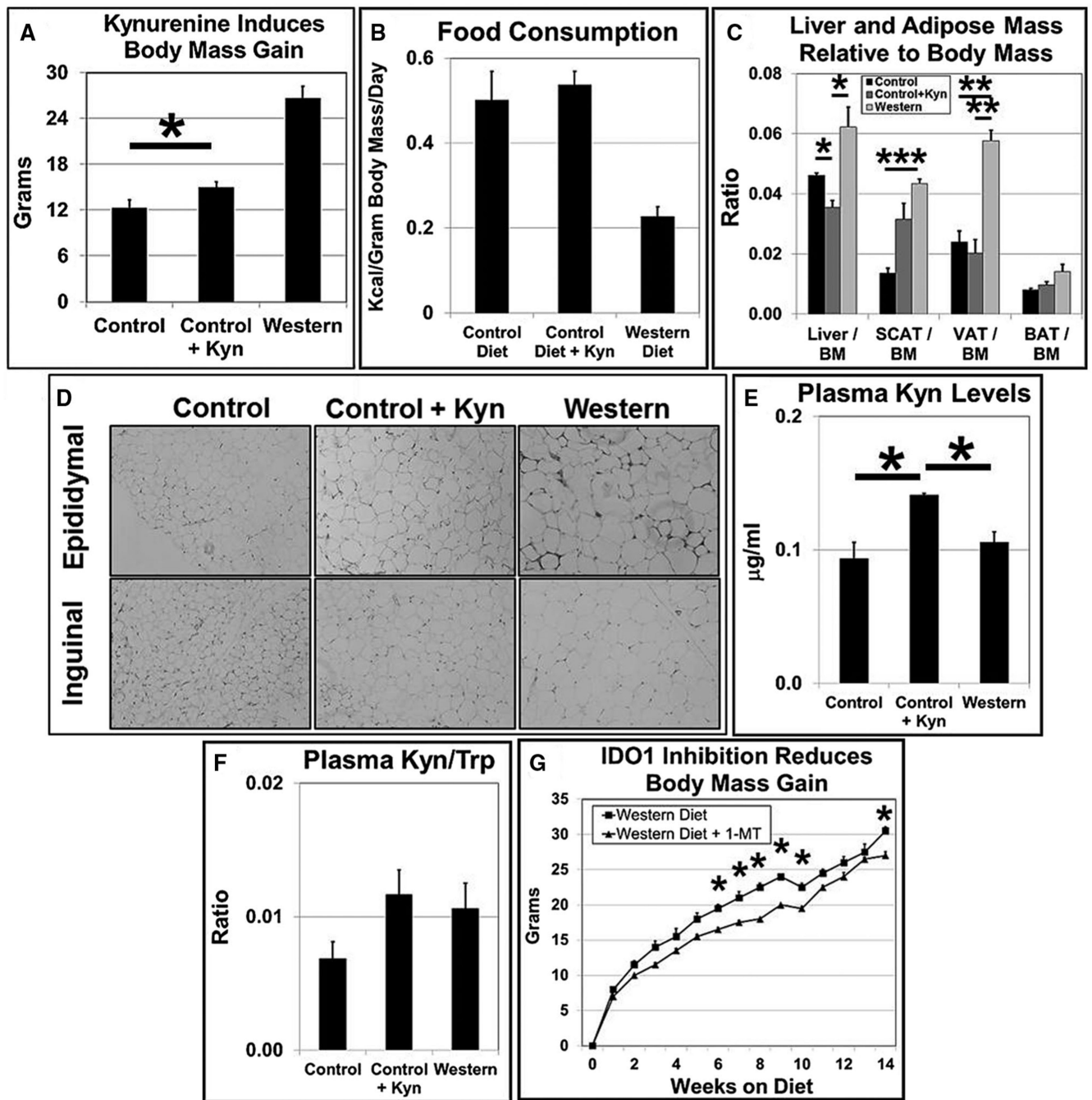
Figure 1.

Kynurenine (Kyn) induces body mass gain primarily in the subcutaneous fat depot. (**A**) Male B6 mice ($n = 6$ mice/experimental group) were fed low-fat control, control+Kyn, or Western diets ad libitum for 20 weeks beginning at weaning. (**B**) Food consumption for each experimental group ($n = 4$) was determined over a 10- to 14-day period beginning at week 15 during the 20-week diet regimen. (**C**) Liver, subcutaneous adipose tissue (SCAT), gonadal or visceral adipose tissue (VAT), and brown adipose tissue (BAT) mass/body mass (BM) ratios were determined at the end of the 20-week diet regimen ($n = 6$/experimental

group). (**D**) Representative sections ($n = 3$) of epididymal (VAT) and inguinal (SCAT) adipose tissue stained with hematoxylin and eosin at termination of the 20-week diet regimen. (**E**) Kyn levels and (**F**) Kyn to tryptophan (Trp) ratios in plasma were determined by HPLC at termination of the 20-week diet regimen ($n = 3$). (**G**) Male B6 mice ($n = 3$ mice/experimental group) were given water ± 1-methyl-L-tryptophan (1MLT, 5 mg/mL) ad libitum for 14 weeks beginning at weaning. *P 0.05, **P 0.01, ***P 0.001. Error bars represent SEM. IDO1, indole-2,3-dioxygenase 1.
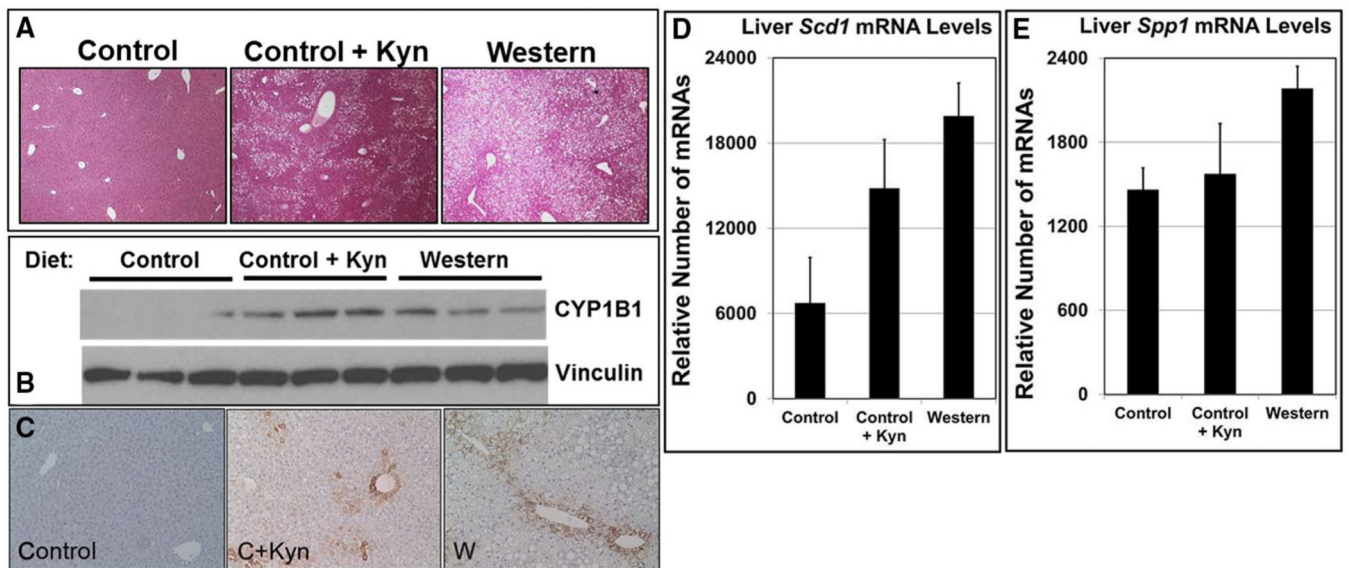
Figure 2.
Kynurenine (Kyn) causes fatty liver and induces hepatic perivenous CYP1B1 expression. Male B6 mice ($n = 6$ mice/experimental group) were fed low-fat control (C), control+Kyn (C+Kyn), and Western (W) diets ad libitum for 20 weeks beginning at weaning. (**A**) Representative sections of liver stained with hematoxylin and eosin at termination of the 20-week diet regimen ($n = 3$). (**B**) Proteins isolated from liver at termination of the 20-week diet regimen were resolved by Western blotting. Vinculin served as a loading control ($n = 3$). (**C**) Liver sections stained with anti-CYP1B1 antibody. Total RNA from liver was subjected to microarray analysis to determine the differential mRNA levels of (**D**) *Scd1* and (**E**) *Spp1* at termination of the 20-week diet regimen ($n = 3$). Error bars represent SEM.
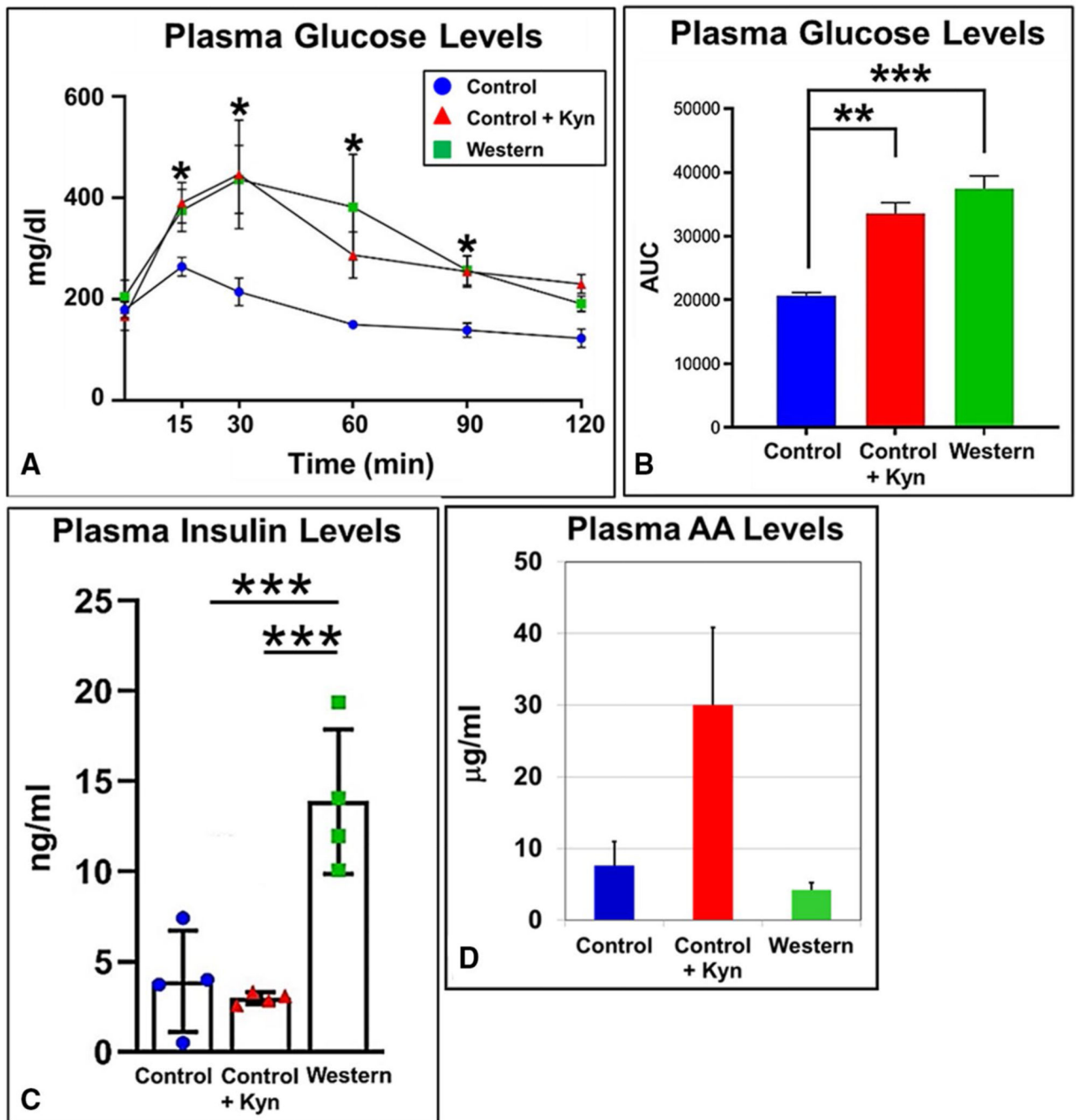
Figure 3.

Kynurenine (Kyn) treatment causes hyperglycemia and decreased plasma insulin levels. Male B6 mice (n = 6 mice/experimental group) were fed low-fat control, control+Kyn, and Western diets ad libitum for 20 weeks beginning at weaning. The mice (n = 6) were fasted for 6 hours, and "/>plasma glucose levels were (**A**)measured at the indicated time points following administration of an oral bolus of glucose (2 g/kg body mass) and (**B**) quantified by calculation of the area under the curve (AUC). (**C**) Insulin plasma levels from the same mice (n = 6) fasted for 6 hours using blood taken by cardiac puncture at sacrifice. (**D**)

Plasma arachidonic acid (AA) concentrations were determined by HPLC from the same mice ($n = 4$). $*P$ 0.05, $**P$ 0.01, $***P$ 0.001. Error bars represent SEM.
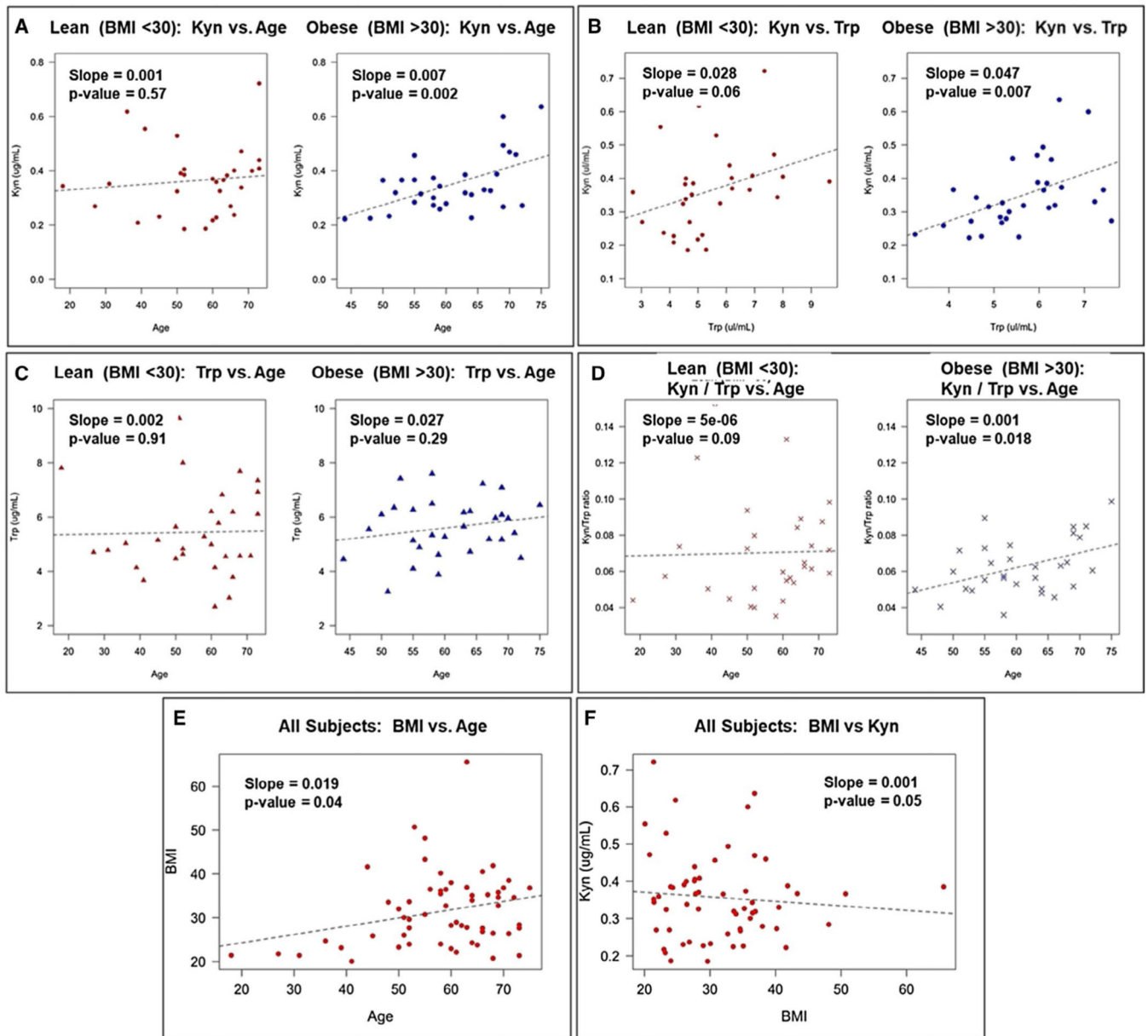
Figure 4.
Kynurenine (Kyn) plasma levels are dependent on age in women with obesity but not lean women. Kyn and tryptophan (Trp) plasma levels and BMI were determined for 60 human females aged 18 to 75. (**A**) Age and Kyn plasma levels were plotted for lean/overweight women (BMI = 19 to < 30) (left panel) and women with obesity (BMI 30) (right panel). (**B**) Plasma Trp and Kyn levels were plotted for lean/overweight women (left panel) and women with obesity (right panel). (**C**) Plasma Trp levels and age were plotted for lean/overweight women (left panel) and women with obesity (right panel). (**D**) Plasma Kyn/Trp ratio and age were plotted for lean/overweight women (left panel) and women with obesity (right panel). (**E**) BMI and age and (**F**) plasma Kyn levels and BMI were plotted for all 60 patients.

TABLE 1

Differential mRNA levels (fold-change) of PPARα-target genes in mouse liver

Gene	Gene product function	Control + kynurenine diet/control diet[a]	Western diet/control diet[a]
Elovl5	Elongates long fatty acids	1.72	NC
G0s2	Regulates adipocyte lipase and lipolysis	2.19	2.18
Retsat	Modulates lipid metabolism and adiposity	1.55	1.65
Scd1	Catalyzes monounsaturated fatty acids	2.42	2.60

NC, no significant change.

[a]Microarray results (P 0.05) for male B6 mice ($n = 3$/experimental group) on a 20-week, ad libitum diet regimen.

TABLE 2

Kynurenine induces lipid metabolic pathways

Cellular pathway	Gene count	P value
Lipid metabolic process	11	0.000103
Negative regulation of transcription from RNA Pol II promoter	13	0.000287
Fatty acid biosynthetic process	5	0.000528
Response to glucose	5	0.000644
Cellular response to insulin stimulus	5	0.001014
Fatty acid metabolic process	6	0.001148
Rhythmic process	5	0.003983
Transcription, DNA-templated	19	0.005534
Metabolic process	8	0.008810
Cellular response to glucose starvation	3	0.009943
Liver development	4	0.012230
Adipose tissue development	3	0.012658

Predicted affected cellular pathways based on differential mRNA expression levels of the 100 most altered genes from male B6 mice on a 20-week regimen of control + kynurenine versus control diets (n = 3/experimental group).

TABLE 3

Shared commonly expressed genes comprising the predicted GO:0055114~oxidation reduction pathway ($P = 0.035$) from liver of male B6 mice on a 20-week diet regimen of Western (W)/control (C) and C+kynurenine (Kyn)/C

Gene	Gene name	Function	W/C	C+Kyn/C
Scd1	Stearoyl-coenzyme A desaturase 1	An integral membrane protein located in the endoplasmic reticulum. SCD1 utilizes O(2) and electrons from reduced cytochrome B5 to introduce the first double bond into saturated fatty acyl-CoA substrates. Contributes to the biosynthesis of membrane phospholipids, cholesterol esters, and triglycerides.	2.60	2.42
Steap4	STEAP family member 4	STEAP (six transmembrane epithelial antigen of prostate) proteins reside in the golgi apparatus. A metalloreductase that reduces Fe(3+) to Fe(2+) and Cu(2+) to Cu(1+), using NAD(+) as acceptor.	1.80	1.65
Retsat	Retinol saturase (all-trans-retinol 13,14 reductase)	Catalyzes the saturation of all-trans-retinol to all-trans-13,14-dihydroretinol.	1.65	1.55
Hsd17b10	Hydroxysteroid (17-beta) dehydrogenase 10	A mitochondrial protein that catalyzes the oxidation of a wide variety of fatty acids and steroids; also a subunit of mitochondrial ribonuclease P, which is involved in tRNA maturation.	2.06	1.49
Ehhadh	Enoyl-coenzyme A, hydratase/3-hydroxyacyl coenzyme A dehydrogenase	One of the four enzymes of the peroxisomal beta-oxidation pathway. The N-terminal region of the encoded protein contains enoyl-CoA hydratase activity, whereas the C-terminal region contains 3-hydroxyacyl-CoA dehydrogenase activity.	2.39	1.46
Ndufb6	NADH dehydrogenase (ubiquinone) 1 beta subcomplex, 6	A subunit of the multisubunit NADH:ubiquinone oxidoreductase (complex I, the first enzyme complex in the electron transport chain composed of 45 different subunits). An inner mitochondrial membrane protein that has NADH dehydrogenase activity and oxidoreductase activity. Transfers electrons from NADH to the respiratory chain, in which the immediate electron acceptor is believed to be ubiquinone.	1.32	1.38
Ndufb2	NADH dehydrogenase (ubiquinone) 1 beta subcomplex, 2	An inner mitochondrial membrane protein that has NADH dehydrogenase activity and oxidoreductase activity. It plays an important role in transferring electrons from NADH to the respiratory chain.	1.27	1.32
Ndufs5	NADH dehydrogenase (ubiquinone) Fe-S protein 5; cDNA sequence BC002163	This gene is a member of the NADH dehydrogenase (ubiquinone) iron-sulfur protein family. The protein is a subunit of the NADH:ubiquinone oxidoreductase (complex I).	1.31	1.30
Ndufa7	NADH dehydrogenase (ubiquinone) 1 alpha subcomplex, 7 (B14.5a)	Complex I functions in the transfer of electrons from NADH to the respiratory chain.	1.27	1.27
Ndufb9	NADH dehydrogenase (ubiquinone) 1 beta subcomplex, 9	Complex I functions in the transfer of electrons from NADH to the respiratory chain.	1.28	1.26
Ndufc1	NADH dehydrogenase (ubiquinone) 1, subcomplex unknown, 1	A subunit of the NADH:ubiquinone oxidoreductase (complex I).	1.25	1.18
Txnl1	Thioredoxin-like 1	Involved in endocytosis and in protection against glucose deprivation–induced cytotoxicity.	0.87	0.86
Alox12E	Arachidonate lipoxygenase, epidermal	The enzyme is implicated in preventing diabetes, adipose dysfunction, obesity, atherosclerosis, and steatohepatitis.	0.75	0.84
Loxl4	Lysyl oxidase-like 4	Essential to the biogenesis of connective tissue, encoding an extracellular copper-dependent amine oxidase that catalyzes the first step in the formation of crosslinks in collagens and elastin.	0.81	0.84
Fa2h	Fatty acid 2-hydroxylase	Catalyzes the synthesis of 2-hydroxysphingolipids, a subset of sphingolipids that contain 2-hydroxy fatty acids.	0.84	0.82
Hsd3b1	Hydroxy-delta-5-steroid dehydrogenase, 3 beta- and steroid delta-isomerase 1	Catalyzes the oxidative conversion of delta-5–3-beta-hydroxysteroid precursors into delta-4-ketosteroids, which leads to the production of all classes of steroid hormones. Also catalyzes the interconversion of 3-beta-hydroxy- and 3-keto-5-alpha-androstane steroids.	0.74	0.79

Gene	Gene name	Function	W/C	C+Kyn/C
Dhrs2	Dehydrogenase/reductase member 2	A member of the short-chain dehydrogenases/reductases (SDR) family, which has over 46,000 members. Members of this family are enzymes that metabolize many different compounds, such as steroid hormones, prostaglandins, retinoids, lipids, and xenobiotics.	0.78	0.78
Kcnab3	Potassium voltage-gated channel, shaker-related subfamily, beta member 3	A member of the potassium channel, voltage-gated, shaker-related subfamily. The encoded protein is one of the beta subunits, which are auxiliary proteins associated with functional Kv-alpha subunits.	0.76	0.74
Cyp24a1	Cytochrome P450, family 24, subfamily a, polypeptide 1	A mitochondrial monooxygenase that initiates the degradation of 1,25-dihydroxyvitamin D3, the physiologically active form of vitamin D3, by hydroxylation of the side chain.	0.80	0.73
Mthfd2	Methylenetetrahydrofolate dehydrogenase (NAD+dependent), methenyltetrahydrofolate cyclohydrolase	A nuclear-encoded mitochondrial bifunctional enzyme with methylenetetrahydrofolate dehydrogenase and methenyltetrahydrofolate cyclohydrolase activities. A homodimer unique in the absolute requirement for magnesium and inorganic phosphate to allow binding of NAD.	0.76	0.70
Wwox	WW domain-containing oxidoreductase	A member of the short-chain dehydrogenases/reductases (SDR) protein family. Disruption causes impaired steroidogenesis, additionally suggesting a metabolic function for the protein.	0.59	0.68

TABLE 4

Expression of genes (fold-change) in liver of male B6 mice ($n = 3$) on a 20-week diet regimen of Western (W)/ control (C) and C + kynurenine (Kyn)/C

Gene	W/C	C+Kyn/C
Positive regulation of insulin secretion		
BGLAP2	NC	0.85
CAPN10	0.52	0.68
CASR	NC	0.81
GJA1	NC	0.72
GLUl	0.48	0.75
ISL1	NC	0.74
PPARD	NC	0.80
Insulin-responsive genes		
AKT2	0.44	NC
GCK	NC	2.73
GHR	1.32	NC
LPIN1	NC	1.70
PAK1	1.65	NC
PCK1	0.42	NC
PKLR	NC	2.72
STAT1	2.73	NC
Response to glucose		
APOA2	NC	1.09
CDKN1B	NC	1.90
EGR1	NC	2.10
LPL	2.77	0.58
PKLR	NC	2.72
SLC37A4	NC	1.36
TXNIP	NC	1.67
Glucose homeostasis		
GCK	NC	2.73
FOXA3	NC	1.50
NUCKS1	0.74	1.25
PIK3R1	1.65	1.55
Cellular response to glucose stimulus		
AACS	NC	4.03
APOC3	1.11	1.12
ERN1	NC	1.30
IGF1	0.69	1.32
POLG	1.27	1.25
XBP1	NC	1.64
Cellular response to glucose starvation		

Gene	W/C	C+Kyn/C
ASNS	0.44	0.49
ATG14	NC	1.28
GCK	NC	2.73
TBL2	NC	1.31
XBP1	NC	1.64
Inflammatory response genes		
AIF1	1.92	NC
ANXA1	1.59	NC
CAMK1D	0.54	NC
CCL5	2.81	NC
CCL6	2.28	NC
CCR2	1.55	NC
CCR5	1.92	NC
CD5L	1.96	NC
CLEC7A	3.74	NC
CXCL1	2.58	NC
CXCL10	6.31	NC
CXCL2	1.56	NC
CXCL9	11.60	NC
IGFBP4	0.50	NC
LY86	1.98	NC
NAIP5	1.63	NC
PLA2G7	2.42	NC
PLGRKT	1.98	NC
PYCARD	2.14	NC
THBS1	3.24	NC
THEMIS2	1.85	NC
TLR1	2.62	NC
TLR2	1.99	NC
TNFRSF21	2.03	NC
Cholesterol		
DHCR7	0.56	NC
FDPS	0.26	NC
HMGCR	0.55	NC
HMGCS1	0.63	NC
HSD17B7	0.62	NC
IDI1	0.19	NC
LSS	0.63	NC
NSDHL	0.36	NC
PMVK	0.44	NC
TM7SF2	0.24	NC
Fatty acid metabolism genes		

Gene	W/C	C+Kyn/C
AACS	NC	4.03
ACACA	0.69	NC
ACACB	NC	1.95
CD36	5.60	NC
ELOVL5	NC	1.72
ELOVL6	1.88	NC
FADS1	0.61	NC
GHR	1.32	NC
HACD3	0.62	NC
LPL	2.77	0.58
SCD1	2.60	2.42
SCD2	2.48	NC
Lipid metabolic process		
ACER1	0.76	0.83
ADIPOR2	1.27	1.33
ALOX12E	0.75	0.84
ANGPTL3	1.37	1.19
APOC3	1.11	1.12
CERS4	0.75	0.81
EHHADHE	2.39	1.46
FA2H	0.84	0.82
MOGAT2	0.73	0.73
MTMR1	0.70	0.68
PLA2G2F	0.75	0.78
PNLIPRP2	0.65	0.65
PTPN11	0.85	0.79
SCD1	2.60	2.42
SCD2	2.48	NC
TNXB	1.48	.49

Gray coloring indicates genes up- or downregulated by both W and C+Kyn compared with C.

NC, no significant change.